The continuous strength method for structural stainless steel design

S. Afshan

Department of Civil and Environmental Engineering, Imperial College London, SW7 2AZ, UK

sheida.afshan06@imperial.ac.uk

L. Gardner

Department of Civil and Environmental Engineering, Imperial College London, SW7 2AZ, UK

leroy.gardner@imperial.ac.uk

Abstract: Current stainless steel design standards are based on elastic, perfectly plastic material behaviour providing consistency with carbon steel design expressions, but often leading to overly conservative results, particularly in the case of stocky elements. More economic design rules in accordance with the actual material response of stainless steel, which shows a rounded stress-strain curve with significant strain hardening, are required. Hence, the continuous strength method (CSM) was developed. The CSM replaces the concept of cross-section classification with a cross-section deformation capacity and replaces the assumed elastic, perfectly plastic material model with one that allows for strain hardening. This paper summarises the evolution of the method and describes its recent simplified form, which is now suitable for code inclusion. Comparison of the predicted capacities with over 140 collected test results shows that the CSM offers improved accuracy and reduced scatter relative to the current design methods. The reliability of the approach has been demonstrated by statistical analyses and the CSM is currently under consideration for inclusion in European and North American design standards for stainless steel structures.

Keywords:
Continuous strength method; Cross-section classification; Cross-section resistance; Local buckling; Reliability analysis; Stainless steel; Strain hardening

1. Introduction

Stainless steel is being increasingly used as a construction material in various structural applications, taking advantage of its well known corrosion resistance, fire resistance and material properties. Given the high initial material costs of stainless steel, associated primarily with its alloying elements, it is essential that its distinctive properties are recognised in the development of structural design rules. This paper focuses on key characteristics of

stainless steels' material stress-strain behaviour, in particular strain hardening, and its implications on structural design. Unlike carbon steel which has an elastic response, with a clearly defined yield point, followed by a yield plateau and a moderate degree of strain hardening, stainless steel has predominantly non-linear stress-strain behaviour with significant strain hardening. The current generation of international stainless steel design standards [1, 2] have been developed largely in line with carbon steel design guidelines, which are based on the idealised elastic, perfectly plastic material behaviour, hence neglecting the beneficial strain hardening effects.

The continuous strength method (CSM) is a newly developed design approach, providing consistency with the observed stainless steel stress-strain response and allowing for strain hardening. The CSM replaces the concept of cross-section classification, which is the basis for the treatment of local buckling in the current design standards for metallic materials such as carbon steel, stainless steel and aluminium alloys, with a non-dimensional measure of cross-section deformation capacity. Background to the method and detailed descriptions of its development over the past decade are published in [3-5]. More recent advancements and simplifications of the CSM, including its extension to carbon steel design may also be found in [6, 7].

The application of the CSM to stainless steel structures, incorporating its recent modifications, is described in this paper. Test data on stainless steel stub columns and beams have been used to generate a simple and continuous relationship between cross-section slenderness and cross-section deformation capacity, referred to as the design base curve. An elastic, linear hardening material model, enabling exploitation of strain hardening, is also described. Although the scope of the CSM is not limited to specific structural loading cases, cross-section capacities in compression and bending are the primary focus of this paper.

2. Current codified treatment of local buckling

The concept of cross-section classification is the current codified approach for the treatment of local buckling in metallic sections and is used to determine the appropriate structural design resistance. The method is most suitable for materials with a stress-strain response resembling the idealized elastic-perfectly plastic material model, where the presence of a clearly defined yield point allows cross-sections to be set into discrete behavioural classes. EN 1993-1-4 [1] adopts the carbon steel cross-section classification approach set out in EN

1993-1-1 [8], with the yield stress f_y taken as the 0.2% proof stress $\sigma_{0.2}$. A series of limits for the width-to-thickness ratios (b/t), in terms of the material properties $\varepsilon = [(235/f_y)(E/210000)]^{0.5}$, edge support conditions (i.e. internal or outstand) and the form of the applied stress field, are provided. The overall cross-section classification is assumed to relate to that of its most slender constituent element, thus neglecting the benefits of element interaction.

Slenderness limits are generally derived on the basis of experimental results at the cross-section level. Owing to the relatively recent emergence of stainless steel as a structural material, the current cross-section classification limits in EN 1993-1-4 [1] were derived on the basis of a limited number of test data. Analysis of results by Gardner and Theofanous [5], based on a more comprehensive experimental database, has shown that the current classification limits are unduly conservative and may in many cases, be relaxed; where possible it was proposed [5] that the stainless steel slenderness limits be harmonised with those for carbon steel.

Analyses of experimental results from stub column and in-plane bending tests have shown a significant conservatism in EN 1993-1-4 [1] rules which limit the cross-section compression resistance to the yield load and the cross-section bending resistance to the plastic moment capacity. Figure 1 shows the results of stub column tests on stainless steel SHS, RHS, angle sections, lipped channel sections and I-sections [9-22]. The test ultimate load N_u has been normalised by the cross-section yield load – determined as the product of the gross cross-sectional area A and the material 0.2% proof stress $\sigma_{0.2}$ – and plotted against the cross-section slenderness $\bar{\lambda}_p$. Figure 2 shows the results of bending tests on stainless steel SHS, RHS and I-sections [10, 12, 13, 15, 20, 23-28] where the test ultimate moment M_u has been normalised by the plastic moment capacity M_{pl} – determined as the product of the section plastic modulus W_{pl} and the material 0.2% proof stress $\sigma_{0.2}$ – and plotted against the cross-section slenderness $\bar{\lambda}_p$.

The slenderness $\bar{\lambda}_p$ has been taken as the cross-section slenderness making due allowance for element interaction in sections comprised of plate assemblies, as explained in Section 3.1.1. The occurrence of strength enhancements induced during manufacturing of cold-formed sections is well-known and predictive models [29-31] have been developed to determine these strength increases. Hence, for the comparisons shown in Figures 1 and 2, in order to

demonstrate the increases in cross-section resistances in compression and bending due to strain hardening effects under load only, and not during section forming, the cross-section weighted average 0.2% proof stress, allowing for the strength enhancements in the corner regions and flat faces of cold-formed sections as recommended in [30] has been employed.

The collected results shown in Figures 1 and 2 clearly reveal significant under-prediction of the capacity of stocky cross-sections due to the lack of allowance for strain hardening. The continuous strength method, described in the following sections, is proposed to address this shortcoming.

3. Development of the continuous strength method

The continuous strength method (CSM) is a strain based design approach featuring two key components – (1) a base curve that defines the level of strain that a cross-section can carry in a normalised form and (2) a material model, which allows for strain hardening and, in conjunction with the strain measure, can be used to determine the cross-section resistance.

3.1 Design base curve

A fundamental feature of the CSM is relating the cross-section resistance to the cross-section deformation capacity, which is controlled by the cross-section slenderness and its susceptibility to local buckling effects. The cross-section deformation capacity determines the ability of the section to advance into the strain hardening region and hence sustain increased loading. A design base curve, providing a continuous relationship between the normalised cross-section deformation capacity and the cross-section slenderness, has been established on the basis of both stub column test data and beam test data.

3.1.1 Cross-section slenderness definition

Within the CSM, the cross-section slenderness is defined in non-dimensional form as the square root of the ratio of the yield stress f_y to the elastic buckling stress of the section. For structural sections consisting of a series of interconnected plates, the elastic buckling stress of the full cross-section $\sigma_{cr,cs}$, allowing for element interaction, may be determined by means of existing numerical [32] or approximate analytical methods [33]. This approach is used in the Direct Strength Method (DSM) [34] and also adopted in the analysis performed herein. This cross-section slenderness definition is given by Eq. (1) and will initially relate to the

centreline dimensions. To maintain consistency with the codified slenderness definitions in [1, 35], which is based on the flat element widths, the resulting slenderness values can be multiplied by the maximum flat to centreline width ratio $(c_{flat}/c_{cl})_{max}$ of the section as given by Eq. (2)

Alternatively, as recommended in EN 1993-1-4 [1] and EN 1993-1-5 [35], the section elastic buckling stress may be taken as the lowest of those of its individual plate elements $\sigma_{cr,p,min,}$ resulting in the section slenderness definition given in Eq. (3). In Eq. (3), $\bar{b}$ is element width, t is the thickness, ε is the material factor and k_σ is the appropriate buckling coefficient, taking due account of the plate support conditions and the applied stress distribution, as outlined in EN 1993-1-5 [35], of the plate element with the lowest elastic buckling stress.

$$\bar{\lambda}_p = \sqrt{\frac{f_y}{\sigma_{cr,cs}}} \qquad \text{based on centreline dimensions} \qquad (1)$$

$$\bar{\lambda}_p = \sqrt{\frac{f_y}{\sigma_{cr,cs}}} \left(\frac{c_{flat}}{c_{cl}}\right) \qquad \text{based on flat widths} \qquad (2)$$

$$\bar{\lambda}_{cs} = \bar{\lambda}_p = \sqrt{\frac{f_y}{\sigma_{cr,p,min}}} = \frac{\bar{b}/t}{28.4\varepsilon\sqrt{k_\sigma}} \qquad (3)$$

3.1.2 Cross-section deformation capacity definition

Cross-section deformation capacity is defined in a normalised format and is taken for stocky sections as the strain at the ultimate load divided by the yield strain. This normalised deformation capacity, referred to as the strain ratio $\varepsilon_{csm}/\varepsilon_y$, can be determined from both stub column and beam test results.

First, the limiting slenderness defining the transition between slender cross-sections (i.e. those that fail due to local buckling below the yield load) and non-slender cross-section (i.e. those that benefit from strain hardening and fail by inelastic local buckling above the yield load) should be defined. This limit may be determined with reference to stainless steel test data shown in Figure 1, equivalent test data for other metallic materials including carbon steel [7] and aluminium alloys [36] and existing Class 3-4 slenderness limits [1, 5, 8].

A linear regression fit to the test data of Figure 1 indicates that, the point on the line where $N_{u,test}/A\sigma_{0.2}$ equals unity occurs at $\bar{\lambda}_p = 0.68$; a similar value is obtained from equivalent carbon steel and aluminium alloy test data. A range of slenderness limits appear in different design standards and research papers. The existing slenderness limits corresponding to the Class 3-4 width-to-thickness ratio (shown in brackets) are: for internal compression elements, 0.739 (42ε) [8] for carbon steel, 0.540 (30.7ε) [1] and 0.651 (37ε) [5] for stainless steel; for outstand elements, 0.756 (14ε) [8] for carbon steel, 0.642 (11.9ε) and 0.594 (11ε) for cold-formed and welded stainless steel respectively [1] and 0.756 (14ε) [5] for stainless steel. Based on the complete carbon steel cross-sections, a limit of 0.776 [34] is given by the DSM, but, in conjunction with a higher partial safety factor than recommended in European standards. Considering the available information, to make the transition between slender and non-slender sections a common limit for stainless steel, carbon steel and aluminium alloys, $\bar{\lambda}_p = 0.68$ is adopted. This slenderness value also marks the limit of applicability of the CSM (i.e. $\bar{\lambda}_p < 0.68$), since beyond this limit there is no significant benefit to be derived from strain hardening, and slender sections may be adequately treated by means of the existing effective width method [1, 35] or the DSM [34].

For stub columns where the ultimate test load N_u exceeds the section yield load N_y, the end shortening at the ultimate load δ_u divided by the stub column length L is used to define the failure strain of the cross-section ε_{lb} due to inelastic local buckling – as shown in Figure 3. For compatibility with the adopted simplified material model (see Section 3.2), the deformation capacity ε_{csm} is obtained by subtracting the plastic strain at the 0.2% proof stress (i.e. 0.002) from the actual local buckling strain ε_{lb}, as given in Eq. (4). Expressing the cross-section deformation capacity in a normalised format, by dividing by the defined yield strain ε_y ($=f_y/E$) enables materials of different strength and stiffness to be considered together and be compared.

For sections that fail before reaching their yield load, the deformation response is influenced by elastic buckling and post-buckling behaviour, and the former definition of the local buckling strain is inappropriate and would lead to over predictions of capacity [4]. Hence the ratio of the ultimate load attained to the yield load is used to provide a suitable alternative measure of the strain ratio – as given in Eq. (5). This is also used to define the strain ratio for

slender sections, Eq. (6), where the cross-section slenderness is greater than the specified limit of 0.68.

For $\bar{\lambda}_p \leq 0.68$

$$\frac{\varepsilon_{csm}}{\varepsilon_y} = \frac{\varepsilon_{lb} - 0.002}{\varepsilon_y} = \frac{\delta_u / L - 0.002}{\varepsilon_y} \qquad \text{for } N_u \geq N_y \tag{4}$$

$$\frac{\varepsilon_{csm}}{\varepsilon_y} = \frac{N_u}{N_y} \qquad \text{for } N_u < N_y \tag{5}$$

For $\bar{\lambda}_p > 0.68$

$$\frac{\varepsilon_{csm}}{\varepsilon_y} = \frac{N_u}{N_y} \tag{6}$$

In bending, assuming plane sections remain plane and normal to the neutral axis, there is a linear relationship between strain ε and curvature κ as given by Eq. (7), where y is the distance from the neutral axis. Hence, analogous to the use of stub column tests data, similar definitions of normalised cross-section deformation capacity may be established based on beam test results. The results of 4 point bending tests, which have a region of uniform curvature between the loading points, have been considered herein. For beams where the ultimate moment resistance M_u exceeds the section elastic moment capacity M_{el}, the total curvature at the ultimate moment κ_u multiplied by the distance from the neural axis to the extreme compressive fibre in the cross-section y_{max} is used to define the strain at failure due to inelastic local buckling ε_{lb} – see Figure 4. The corresponding strain ratio is obtained following a similar approach to the stub column test results and is given by Eq. (8); κ_{el} is the elastic curvature corresponding to M_{el} and is given as M_{el}/EI, where E is the material Young's modulus and I is the section second moment of area. For sections which fail before reaching their elastic moment capacity, the ratio of the ultimate moment resistance to the section elastic moment capacity is used to define the strain ratio, as given in Eq. (9). The same definition is employed for slender sections, given by Eq. (10). The assumed compressive and bending strain distributions across the cross-section are illustrated for an I-section in Figure 5.

$$\varepsilon = \kappa\, y \tag{7}$$

For $\bar{\lambda}_p \leq 0.68$

$$\frac{\varepsilon_{csm}}{\varepsilon_y} = \frac{\varepsilon_{lb} - 0.002}{\varepsilon_y} = \frac{\kappa_u y_{max} - 0.002}{\kappa_{el} y_{max}} \quad \text{for } M_u \geq M_{el} \tag{8}$$

$$\frac{\varepsilon_{csm}}{\varepsilon_y} = \frac{M_u}{M_{el}} \quad \text{for } M_u < M_{el} \tag{9}$$

For $\bar{\lambda}_p > 0.68$

$$\frac{\varepsilon_{csm}}{\varepsilon_y} = \frac{M_u}{M_{el}} \tag{10}$$

3.1.3 Experimental database and proposed base curve

Test data on stainless steel stub columns and 4 point bending tests from a broad spectrum of existing testing programs [9-15, 19-22, 25, 26] were gathered and combined with equivalent carbon steel data [7] for the development of the design base curve. Using the criteria described above, the test data were plotted on a graph of normalised deformation capacity $\varepsilon_{csm}/\varepsilon_y$ versus cross-section slenderness $\bar{\lambda}_p$, as shown in Figure 6. A continuous function of the general form given by Eq. (11) was then fitted to the test data; this function is similar in form to the established relationship between normalised critical elastic buckling strain $\varepsilon_{cr}/\varepsilon_y$ and plate slenderness for flat plate elements given by Eq. (12), but will differ due to the effects of inelastic buckling, imperfections, residual stresses and post-buckling response. The values of A and B were determined following a regression fit of Eq. (11) to the test data, ensuring that the resulting curve passes through the identified limit between slender and non-slender sections, i.e. (0.68, 1) point, resulting in Eq. (13). Two upper bounds have been placed on the predicted cross-section deformation capacity; the first limit of 15 corresponds to the material ductility requirement expressed in EN 1993-1-1 [8] and the second limit of $0.1\varepsilon_u/\varepsilon_y$, where ε_u is the strain corresponding to the ultimate tensile stress, is related to the adopted stress-strain material model, and ensures no significant over-predictions of the cross-section resistance can occur.

$$\frac{\varepsilon_{csm}}{\varepsilon_y} = \frac{A}{\bar{\lambda}_{cs}^{\,B}}$$

$$\frac{\varepsilon_{cr}}{\varepsilon_y} = \frac{1}{\bar{\lambda}_{cs}^{\,2}}$$

$$\frac{\varepsilon_{csm}}{\varepsilon_y} = \frac{0.25}{\bar{\lambda}_{cs}^{\,3.6}} \quad \text{but} \quad \frac{\varepsilon_{csm}}{\varepsilon_y} \le \min\left(15, \frac{0.1\varepsilon_u}{\varepsilon_y}\right)$$

3.2 Material model

Earlier versions of the CSM utilised the Ramberg-Osgood material model [3-5], which resulted in relatively complex resistance expressions. It was found that similar accuracy could in fact be achieved with simpler material models, and the design expressions become more suitable for structural designers and inclusion in design codes.

The CSM employs an elastic, linear hardening material model. The origin of the adopted material model starts at 0.2% off-set plastic strain, which combined with the strain ratio definitions, provided in Section 3.1.2, predicts the correct corresponding stress. The yield stress point is defined as (f_y, ε_y), where f_y is taken as the material 0.2% proof stress and ε_y is the corresponding elastic strain $\varepsilon_y = f_y/E$, where E is the slope of the elastic region and is taken as the material's Young's modulus. The strain hardening slope is determined as the slope of the line passing through the 0.2% proof stress point (f_y, ε_y+0.002) and a specified maximum point (ε_{max}, f_{max}) with ε_{max} taken as $0.16\varepsilon_u$, where ε_u is the ultimate tensile strain, and f_{max} is taken as the ultimate tensile stress f_u, as given by Eq. (14). The strain at the material ultimate tensile stress ε_u is determined from Annex C of EN 1993-1-4 [1] and is given by Eq. (15). A schematic diagram of the material model employed is shown in Figure 7.

$$E_{sh} = \frac{f_u - f_y}{0.16\varepsilon_u - (\varepsilon_y + 0.002)}$$

$$\varepsilon_u = 1 - \frac{f_y}{f_u}$$

3.3 Cross-section compression and bending resistance

Having established the normalised deformation capacity of the cross-section $\varepsilon_{csm}/\varepsilon_y$ from the design base curve (Equation (13)), the limiting strain ε_{csm} may now be used in conjunction with the proposed elastic, linear hardening material model to determine the cross-section resistances in compression and bending.

For sections with $\bar{\lambda}_p \leq 0.68$, the cross-section compression resistance $N_{c,Rd}$ is given by Eq. (16), where A is the gross cross-sectional area, f_{csm} is the limiting stress determined from the strain hardening material model, resulting in Eq. (17) and γ_{M0} is the material partial safety factor as recommended in EN 1993-1-4 [1].

$$N_{c,Rd} = N_{csm,Rd} = \frac{Af_{csm}}{\gamma_{M0}} \tag{16}$$

$$f_{csm} = f_y + E_{sh}\varepsilon_y\left(\varepsilon_{csm}/\varepsilon_y - 1\right) \tag{17}$$

Assuming that plane sections remain plane and normal to the neutral axis in bending, the corresponding linearly-varying strain distribution may be used in conjunction with the material model to determine the cross-section in-plane bending resistance M_{csm} through Eq. (18), where f is the stress in the section with a maximum outer fibre value of f_{csm}, y is the distance from the neutral axis and dA is the incremental cross-sectional area.

$$M_{csm} = \int_A f\ y\ dA \tag{18}$$

For sections with $\bar{\lambda}_p \leq 0.68$, the cross-section bending resistance $M_{c,Rd}$ is given by Eq. (19) and (20) for major axis and minor axis bending, respectively, where W_{pl} is the plastic section modulus, W_{el} is the elastic section modulus and α is 2.0 for SHS/RHS and 1.2 for I-sections. A detailed description of the derivation of the CSM bending resistance equations is given in [7].

$$M_{y,c,Rd} = M_{y,csm,Rd} = \frac{W_{pl,y}f_y}{\gamma_{M0}}\left[1 + \frac{E_{sh}}{E}\frac{W_{el,y}}{W_{pl,y}}\left(\frac{\varepsilon_{csm}}{\varepsilon_y} - 1\right) - \left(1 - \frac{W_{el,y}}{W_{pl,y}}\right)\Big/\left(\frac{\varepsilon_{csm}}{\varepsilon_y}\right)^2\right] \tag{19}$$

$$M_{z,c,Rd} = M_{z,csm,Rd} = \frac{W_{pl,z} f_y}{\gamma_{M0}} \left[1 + \frac{E_{sh}}{E} \frac{W_{el,z}}{W_{pl,z}} \left(\frac{\varepsilon_{csm}}{\varepsilon_y} - 1 \right) - \left(1 - \frac{W_{el,z}}{W_{pl,z}} \right) \Big/ \left(\frac{\varepsilon_{csm}}{\varepsilon_y} \right)^{\alpha} \right] \quad (20)$$

4. Comparison with test data and design models

The predictions from the method have been compared with experimental results on 81 stainless steel stub columns [9-14, 16-22] and 65 beams [10, 12, 13, 20, 23-28]. It has been shown that the method offers improved mean resistance and reduced scatter compared to the EN 1993-1-4 [1] design rules which are known to be conservative for stocky cross-sections – as illustrated in Figures 8 and 9. Key numerical comparisons, including the mean and the coefficient of variation (COV), of the CSM and the EN 1993-1-4 [1] predictions with the test data are presented in Tables 1 and 2 for the stub columns and the beams, respectively.

5. Reliability analysis

In order to verify the CSM design equations, a standard reliability analysis in accordance with EN 1990 – Annex D [37] was performed and a summary of the key statistical parameters are presented in Tables 3. The following symbols are used: $k_{d,n}$ = design (ultimate limit state) fractile factor for n tests, where n is the population of test data under consideration; b = average ratio of experimental to model resistance based on a least squares fit to the test data; V_δ = coefficient of variation of the tests relative to the resistance model; and V_r = combined coefficient of variation incorporating both model and basic variable uncertainties. The analyses indicate that CSM provides reliable results, with improved mean resistance and considerably lower scatter than the EN 1993-1-4 [1], as also illustrated in Figs. 10 and 11. EN 1993-1-4 (2006) employs a partial safety factor γ_{M0} of 1.1. The results of the reliability analysis show that this value is safe for CSM, and is the recommended value.

6. Worked examples

Two examples are provided in this section to demonstrate the workings of the CSM for the design of stainless steel cross-sections in compression and bending. The design calculations for an I-section in compression and a RHS in bending are presented in Examples I and II, respectively. The geometric and material properties of the tested specimens have been used and all factors of safety have been set to unity, to allow direct comparison with the test results.

Example I: Compression resistance

The CSM predicted compression resistance of I-section 160×80×10×6 stub column, tested in [20], was determined as follows:

Cross-section geometric and material properties:

h = 158.80 mm	t_w = 6.00 mm	E = 198000 N/mm^2	ε_y = 299/198000=0.00151
b = 79.50 mm	Weld size = 4.24 mm	f_y=299 N/mm^2	ε_u = 1-299/610=0.51
t_f = 9.86 mm	A = 2402.22 mm^2	f_u=610 N/mm^2	

Determine cross-section slenderness

$$\bar{\lambda}_p = \sqrt{\frac{f_y}{\sigma_{cr,cs}}} = \sqrt{\frac{299}{1866.85}} = 0.40$$

Multiplying by $(c_{flat}/c_{cl})_{max}$, where c_{flat} is the flat element width and c_{cl} is the centreline element width.

$$0.40 \times 0.877 = 0.35 \, (\leq 0.68 \therefore \text{CSM applies})$$

Determine cross-section deformation capacity:

$$\frac{\varepsilon_{csm}}{\varepsilon_y} = \frac{0.25}{0.35^{3.6}} = 10.85 < \min\left(15, \frac{0.1\varepsilon_u}{\varepsilon_y}\right)$$

Determine the strain-hardening slope:

$$E_{sh} = \frac{f_u - f_y}{0.16\varepsilon_u - (\varepsilon_y + 0.002)} = \frac{610 - 299}{0.16 \times 0.51 - (0.00151 + 0.002)} = 3984 \text{ N/mm}^2$$

Determine the cross-section compression resistance:

$$f_{csm} = f_y + E_{sh}\varepsilon_y\left(\varepsilon_{csm}/\varepsilon_y - 1\right) = 299 + 3984 \times 0.00151(10.85 - 1) = 358.23 \text{ N/mm}^2$$

$$N_{c,Rd} = N_{csm,Rd} = \frac{2402.22 \times 358.23}{1.0} = 860.55 \text{ kN}$$

[Test ultimate load = 885.00 kN; EN 1993-1-4 predicted compression resistance = 718.26 kN]

Example II: In-plane bending resistance

The CSM predicted in-plane bending resistance of RHS 150×100×6 about its major axis, tested in [12], was determined as follows:

Cross-section geometric and material properties:

h = 149.90 mm	r_i = 4.50 mm	W_{el} = 110128 mm^3	f_u=654 N/mm^2
b = 100.20 mm	A = 2714.71 mm^2	E = 193000 N/mm^2	ε_y=367/193000=0.00190
t = 5.85 mm	W_{pl} = 134807 mm^3	f_y=367 (1) N/mm^2	ε_u=1-367/654=0.44

(1) This is the cross-section weighted average yield strength, allowing for corner strength enhancement by means of recommendations in [30].

Determine the cross-section slenderness

$$\bar{\lambda}_p = \sqrt{\frac{f_y}{\sigma_{cr,cs}}} = \sqrt{\frac{367}{3533}} = 0.32$$

Multiplying by $(c_{flat}/c_{cl})_{max}$, where c_{flat} is the flat element width and c_{cl} is the centreline element width.

$$0.32 \times 0.897 = 0.289 \, (\leq 0.68 \therefore \text{CSM applies})$$

Determine the cross-section deformation capacity:

$$\frac{\varepsilon_{csm}}{\varepsilon_y} = \frac{0.25}{0.289^{3.6}} = 21.81 > \min\left(15, \frac{0.1\varepsilon_u}{\varepsilon_y}\right) \quad \therefore \quad \frac{\varepsilon_{csm}}{\varepsilon_y} = 15$$

Determine the strain-hardening slope:

$$E_{sh} = \frac{f_u - f_y}{0.16\varepsilon_u - (\varepsilon_y + 0.002)} = \frac{654 - 367}{0.16 \times 0.44 - \left(0.00190 + 0.002\right)} = 4328 \, \text{N/mm}^2$$

Determine the cross-section in-plane bending resistance:

$$M_{y,c,Rd} = M_{y,csm,Rd} = \frac{W_{pl,y} f_y}{\gamma_{M0}} \left[1 + \frac{E_{sh}}{E} \frac{W_{el,y}}{W_{pl,y}} \left(\frac{\varepsilon_{csm}}{\varepsilon_y} - 1 \right) - \left(1 - \frac{W_{el,y}}{W_{pl,y}} \right) \Big/ \left(\frac{\varepsilon_{csm}}{\varepsilon_y} \right)^2 \right] =$$

$$\frac{367 \times 134808}{1.0} \left[1 + \frac{4328}{193000} \times \frac{110128}{134808} (15 - 1) - \left(1 - \frac{110128}{134808} \right) \Big/ (15)^2 \right] = 62.23 \, \text{kNm}$$

[Test ultimate moment = 70.54 kNm; EN 1993-1-4 predicted bending resistance = 49.41 kNm]

7. Conclusions

The importance of strain hardening in the design of stainless steel structures was highlighted. A newly developed design method called the continuous strength method, providing a rational exploitation of strain hardening was presented. The evolution of the method for stainless steel structures, covering its recent simplifications and refinements, was described in detail. Test data on stainless steel stub columns and in-plane bending tests were used to make comparisons with the predicted results from the proposed method and EN 1993-1-4 guidelines. Reliability analyses were also performed to statistically validate the method for compression and in-plane bending resistance of stainless steel structural sections. It was shown that the method offers improved mean resistance and lower scatter compared to the EN 1993-1-4 provisions, leading to more economical design.

References

[1] EN 1993-1-4. Eurocode 3: Design of steel structures - Part 1-4: General rules - Supplementary rules for stainless steels. Brussels: European Committee for Standardization (CEN); 2006.

[2] AISC Design Guide 30: Structural Stainless Steel. American Institute of Steel Construction; 2012.

[3] Gardner L. A new approach to structural stainless steel design. PhD Thesis. UK: Imperial College London; 2002.

[4] Ashraf M, Gardner L, Nethercot D. Structural stainless steel design: resistance based on deformation capacity. Journal of Structural Engineering, 2008;134(3):402-11.

[5] Gardner L, Theofanous M. Discrete and continuous treatment of local buckling in stainless steel elements. Journal of Constructional Steel Research, 2008;64(11):1207-16.

[6] Gardner L. The continous strength method. Proceedings of the ICE - Structures and Buildings, 2008;161(3):127-33.

[7] Gardner L, Wang F, Liew A. Influence of strain hardening on the behaviour and design of steel structures. International Journal of Structural Stability and Dynamics, 2011;11(5):855-75.

[8] EN 1993-1-1. Eurocode 3: Design of steel structures - Part 1-1: General rules and rules for buildings. Brussels: European Committee for standardization (CEN); 2005.

[9] Kuwamura H. Local buckling of thin-walled stainless steel members. Steel Structures, 2003;3:191-201.

[10] Saliba N, Gardner L. Cross-section stability of lean duplex stainless steel welded I-sections. Journal of Constructional Steel Research, 2013;80:1-14.

[11] Gardner L, Nethercot D. Experiments on stainless steel hollow sections—Part 1: Material and cross-sectional behaviour. Journal of Constructional Steel Research, 2004;60(9):1291-318.

[12] Talja A, Salmi P. Design of stainless steel RHS beams, columns and beam-columns. Research note 1619. Finland. VTT building technology,1995.

[13] Gardner L, Talja A, Baddoo N. Structural design of high-strength austenitic stainless steel. Thin-Walled structures, 2006;44(5):517-28.

[14] Theofanous M, Gardner L. Testing and numerical modelling of lean duplex stainless steel hollow section columns. Engineering Structures, 2009;31(12):3047-58.

[15] Afshan S, Gardner L. Experimental study of cold-formed ferritic stainless steel hollow sections. Journal of Structural Engineering (ASCE), In press.

[16] Young B, Lui WM. Behavior of cold-formed high strength stainless steel sections. Journal of Structural Engineering, 2005;131(11):1738-45.

[17] Young B, Liu Y. Experimental investigation of cold-formed stainless steel columns. Journal of Structural Engineering, 2003;129(2):169-76.

[18] Liu Y, Young B. Buckling of stainless steel square hollow section compression members. Journal of Constructional Steel Research, 2003;59(2):165-77.

[19] ECSC. Work Package 6 WP6. ECSC project—development of the use of stainless steel in construction. Document RT810, Contract No. 7210 SA/ 842. UK: The Steel Construction Institute; 2000.

[20] ECSC. Work Package 2 WP2. ECSC project—development of the use of stainless steel in construction. Document RT810, Contract No. 7210 SA/ 842. UK: The Steel Construction Institute; 2000.

[21] Rasmussen K, Hancock G. Design of cold-formed stainless steel tubular members. I: Columns. Journal of Structural Engineering (ASCE), 1993;119(8):2349-67.

[22] Yuan HX, Wang YQ, Shi YJ, Gardner L. Stub column tests on stainless steel built-up sections. Thin-Walled structures, Special Issue for Experts Seminar, Submitted.

[23] Real E, Mirambell E. Flexural behaviour of stainless steel beams. Engineering Structures, 2005;27(10):1465-75.

[24] Gardner L, Nethercot D. Experiments on stainless steel hollow sections—Part 2: Member behaviour of columns and beams. Journal of Constructional Steel Research, 2004;60(9):1319-32.

[25] Zhou F, Young B. Tests of cold-formed stainless steel tubular flexural members. Thin-Walled structures, 2005;43(9):1325-37.

[26] Rasmussen K, Hancock G. Design of cold-formed stainless steel tubular members. II: Beams. Journal of Structural Engineering (ASCE), 1993;119(8):2368-86.

[27] Theofanous M, Gardner L. Experimental and numerical studies of lean duplex stainless steel beams. Journal of Constructional Steel Research, 2010;66(6):816-25.

[28] Theofanous M, Gardner L. Plastic design of stainless steel structures. International colloquium on stability and ductility of steel structures (SDSS' Rio 2010). Rio de Janeiro, Brazil; 2010. p. 8-10.

[29] Ashraf M, Gardner L, Nethercot D. Strength enhancement of the corner regions of stainless steel cross-sections. Journal of Constructional Steel Research, 2005;61(1):37-52.

[30] Cruise RB, Gardner L. Strength enhancements induced during cold forming of stainless steel sections. Journal of Constructional Steel Research, 2008;64(11):1310-6.

[31] Rossi B, Afshan S, Gardner L. Strength enhancements in cold-formed structural sections – Part II: Predictive models. Journal of Constructional Steel Research, Submitted.

[32] Schafer B, Ádány S. Buckling analysis of cold-formed steel members using CUFSM: conventional and constrained finite strip methods. Eighteenth international specialty conference on cold-formed steel structures; 2006. p. 39-54.

[33] Seif M, Schafer BW. Local buckling of structural steel shapes. Journal of Constructional Steel Research, 2010;66(10):1232-47.

[34] Schafer BW. Review: the direct strength method of cold-formed steel member design. Journal of Constructional Steel Research, 2008;64(7):766-78.

[35] EN 1993-1-5. Eurocode 3: Design of steel structures - Part 1-5: Plated structural elements. Brussels: European Committee for standardization (CEN); 2006.

[36] Su MN, Young B, Gardner L. Compression tests of alluminium alloy cross-sections. Fourteenth international symposium on tubular structures (ISTS 14). London, UK; 2012. p. 501-8.

[37] EN 1990. Eurocode - Basis of structural design. Brussels: European Committee for Standardization (CEN); 2002.

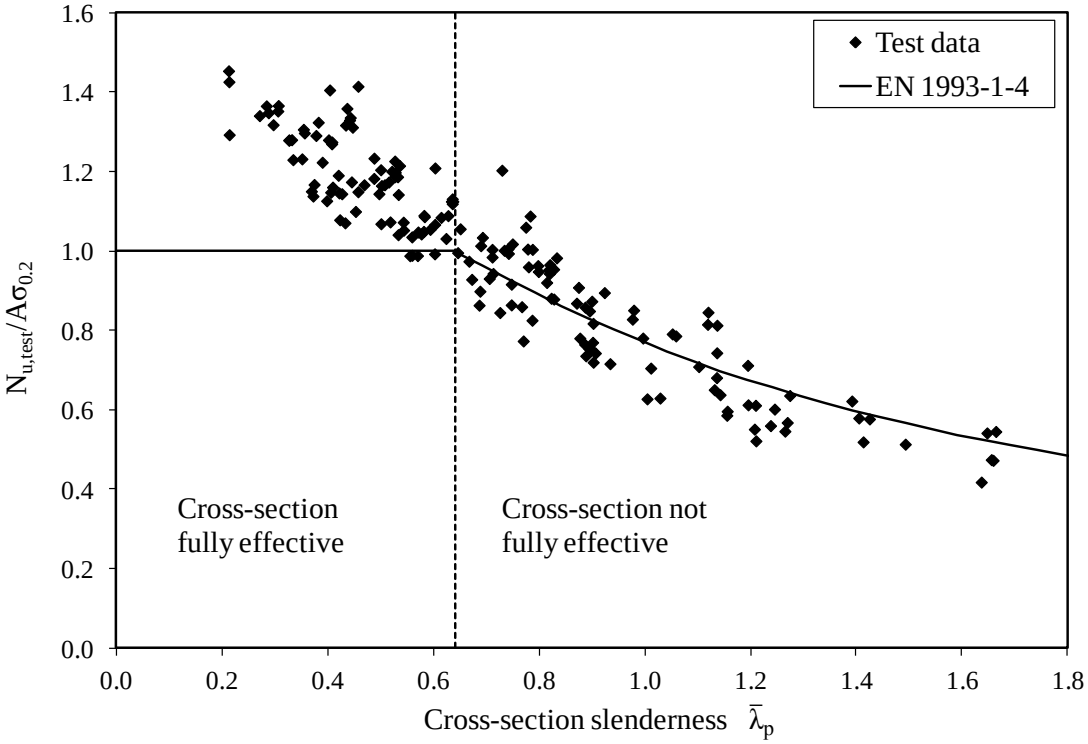

Fig. 1. Comparison of 81 stub column test results with EN 1993-1-4 provisions.

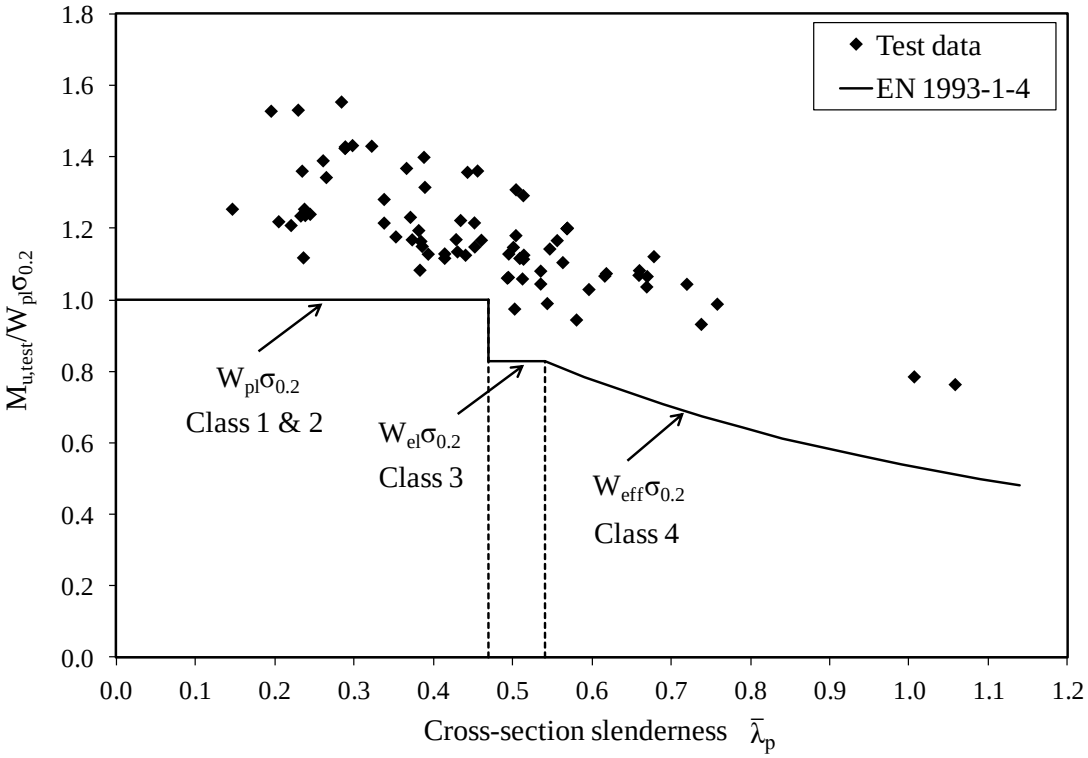

Fig. 2. Comparison of 65 beam test results with EN 1993-1-4 provisions.

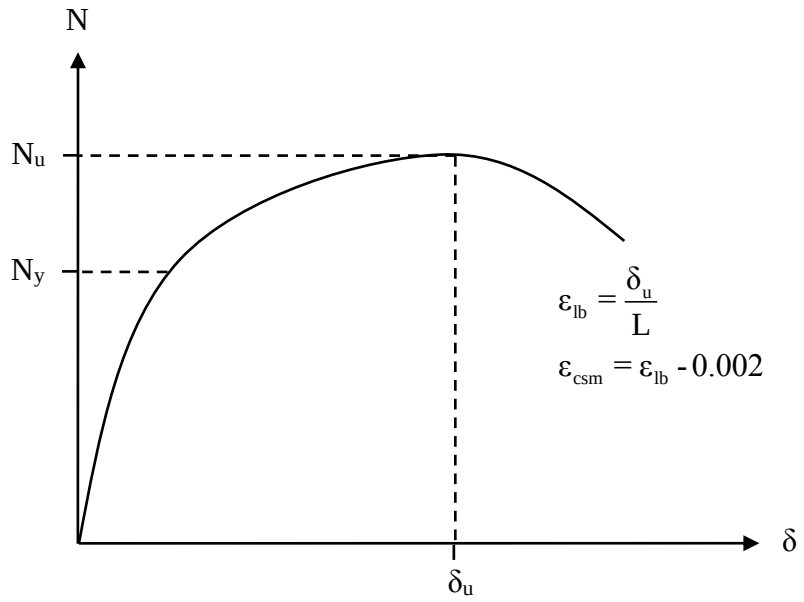

Fig. 3. Stub column load end-shortening response ($N_u > N_y$).

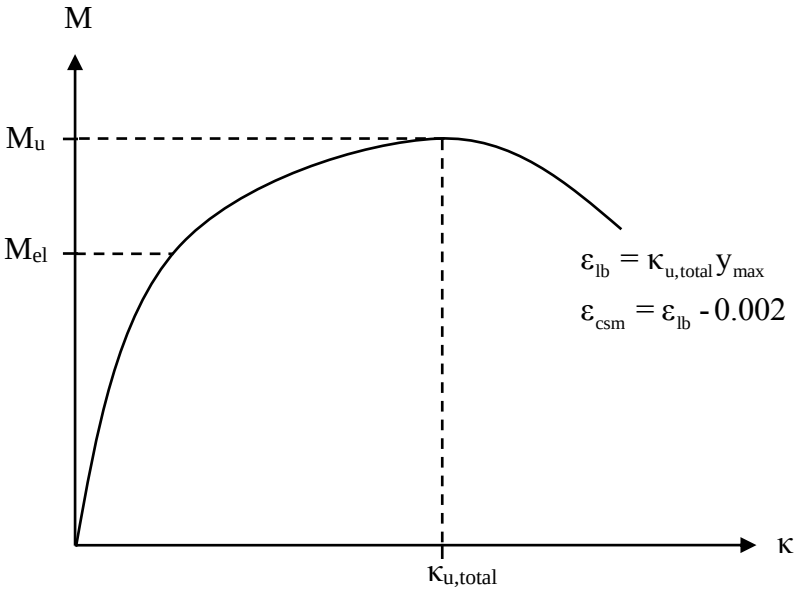

Fig. 4. Beam moment-curvature response ($M_u > M_{el}$).

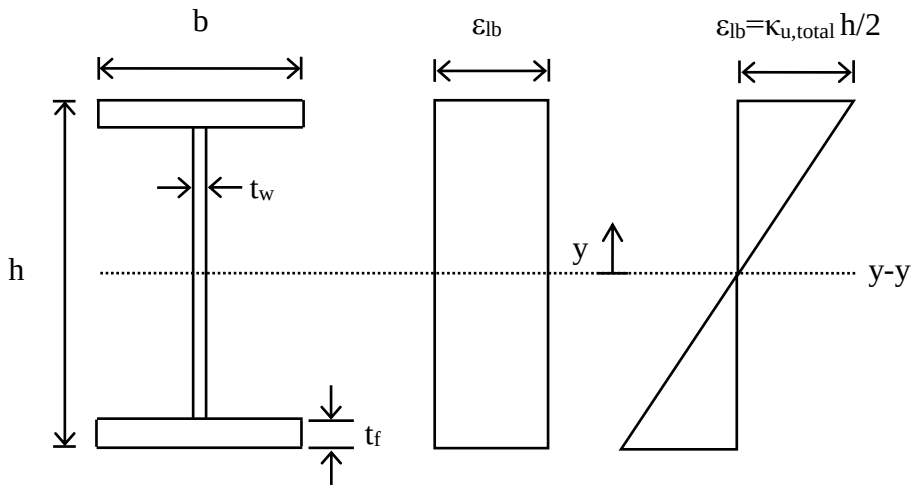

Fig. 5. (a). I-section geometry (b). Uniform compressive strain distribution (c). Pure bending strain distribution.

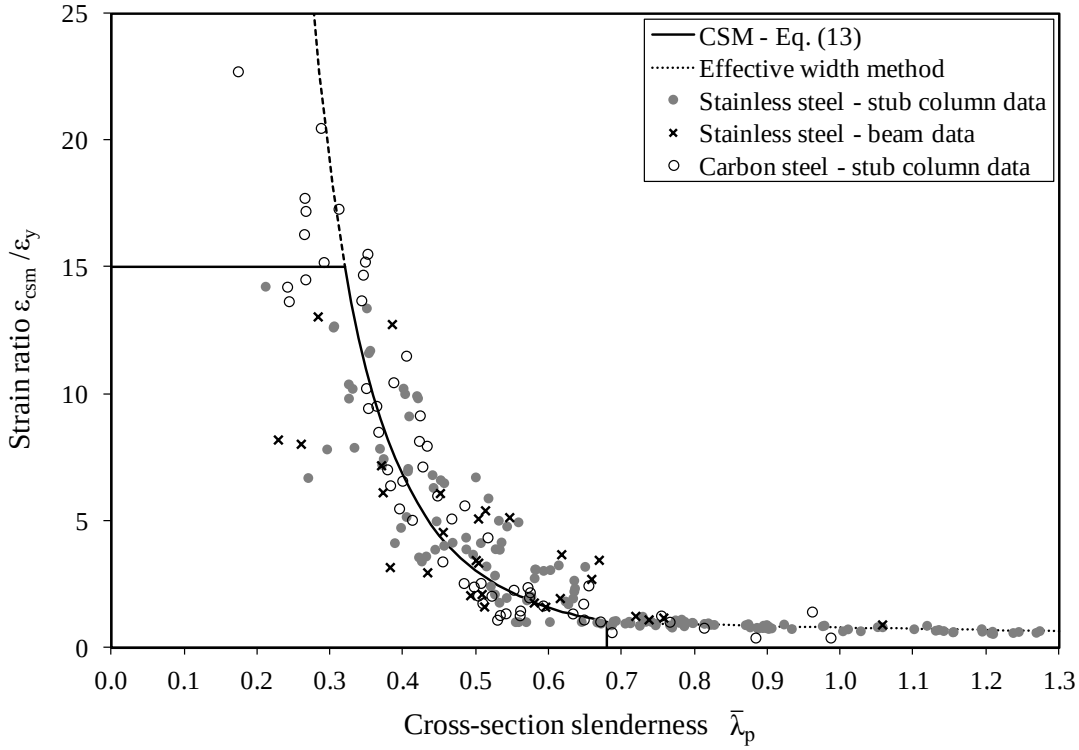

Fig. 6. Base curve – relationship between strain ratio and slenderness.

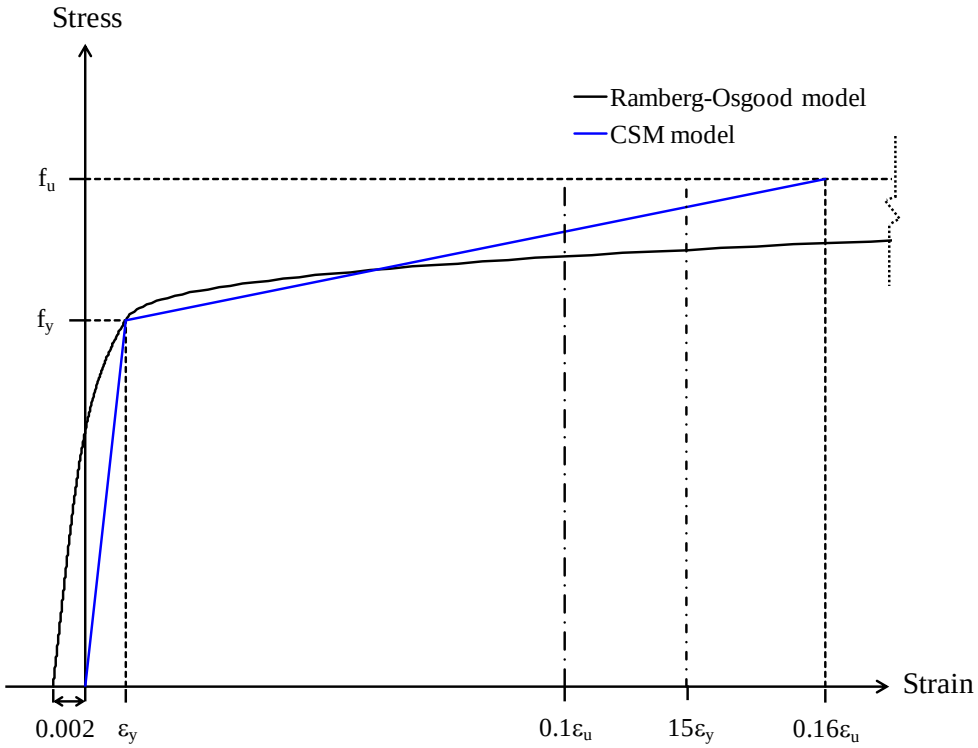

Fig. 7. CSM elastic, linear hardening material model.

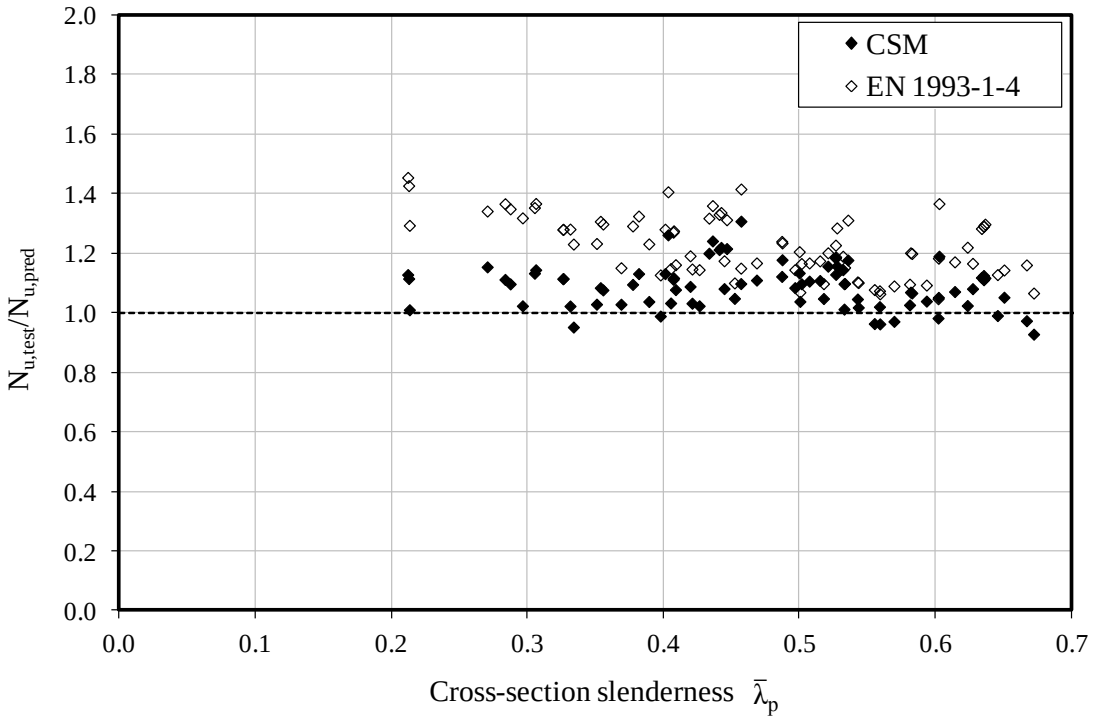

Fig. 8. Comparison of the stub column tests with the CSM and EN 1993-1-4 predictions.

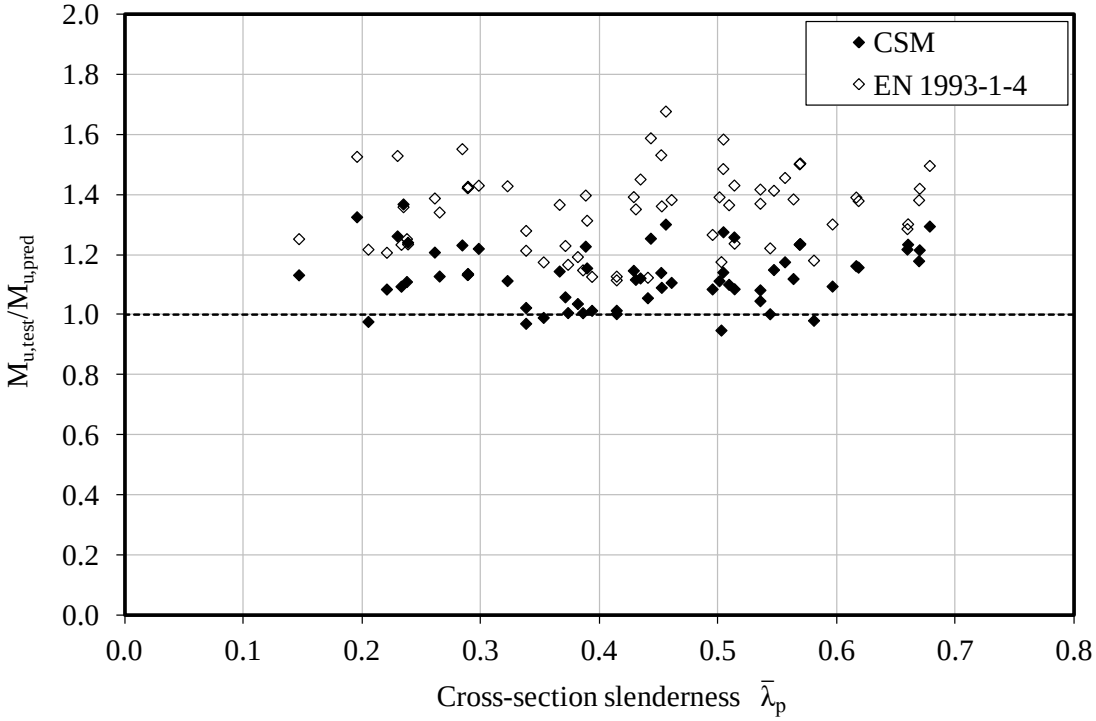

Fig. 9. Comparison of the beam tests with the CSM and EN 1993-1-4 predictions.

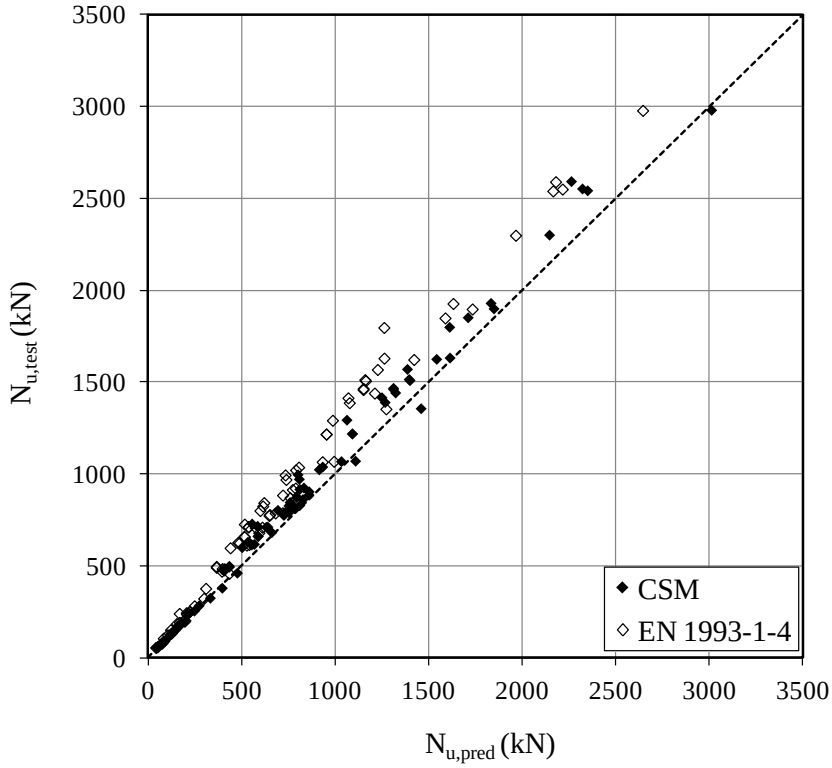

Fig. 10. Experimental and predicted compression resistance.

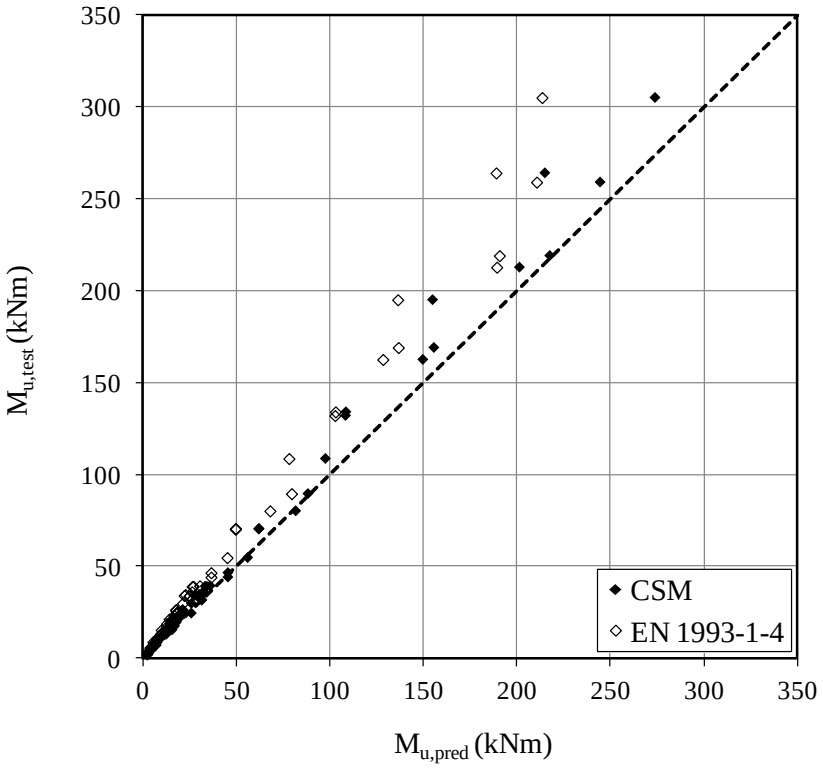

Fig. 11. Experimental and predicted bending resistance.

Table 1

Comparison of the CSM and EN 1993-1-4 predictions with the stub column test results

No. of tests: 81	N_{test}/N_{EC3}	N_{test}/N_{csm}	N_{csm}/N_{EC3}
Mean	1.222	1.088	1.123
COV	0.082	0.069	-

Table 2

Comparison of the CSM and EN 1993-1-4 predictions with the beam test results

No. of tests: 65	M_{test}/M_{EC3}	M_{test}/M_{csm}	M_{csm}/M_{EC3}
Mean	1.351	1.134	1.191
COV	0.098	0.085	-

Table 3

Summary of the CSM reliability analysis results

Test data	n	$k_{d,n}$	b	V_δ	V_r	γ_{M0}
Stub columns	81	3.215	1.075	0.068	0.102	0.96
Beams	65	3.247	1.108	0.086	0.114	0.98